PERGAMON

Available online at www.sciencedirect.com

SCIENCE DIRECT®

Polyhedron 22 (2003) 1973–1980

POLYHEDRON

www.elsevier.com/locate/poly

μSR studies of organic and molecular magnets

Stephen J. Blundell [a,*], Francis L. Pratt [b], Tom Lancaster [a], Ishbel M. Marshall [a], Christopher A. Steer, Sarah L. Heath [c], Jean-François Létard [d], Tadashi Sugano [a,e], Dragan Mihailovic [f], Ales Omerzu [f]

[a] *Oxford University, Department of Physics, Clarendon Laboratory, Parks Road, Oxford OX1 3PU, UK*
[b] *ISIS, Rutherford Appleton Laboratory, Chilton Oxfordshire OX11 0QX, UK*
[c] *University of York, Department of Chemistry, York YO10 5DD, UK*
[d] *ICMCB, Grp. Sci. Mol., UPR CNRS 9048, F-33608 Pessac, France*
[e] *Department of Chemistry, Meiji Gakuin University, Kamikurata, Totsuka-ku, Yokohama 244, Japan*
[f] *Solid State Physics Department, Institute Jozef Stefan, Jamova 39, Ljubljana, Slovenia*

Received 6 October 2002; accepted 10 January 2003

Abstract

Muon-spin rotation and relaxation (μSR) experiments have been performed on a variety of novel organic and molecular magnetic systems. In these experiments, implanted muons are used to study the magnitude, distribution and dynamics of the local field at the muon site. Calculations of the spatial dependence of the dipole-field inside the unit cell are used to interpret the data and determine the muon site in certain cases. We describe and review muon experiments on nitronyl nitroxide organic ferromagnets and antiferromagnets. We discuss a muon study of the spin crossover phenomenon which has been studied in $Fe(PM\text{-}PEA)_2(NCS)_2$, and which shows Gaussian and root-exponential muon relaxation in the high-spin and low-spin phases, respectively. The effects of high temperature annealing on TDAE-C_{60} have also been studied with μSR. Experiments on a disc-shaped molecular complex containing Fe_{19} (with spin 31/2) reveal the effects of fluctuations of magnetization and allow an estimate of the fluctuation rate. These experiments demonstrate the wide range of problems which can be tackled using the μSR technique.

Keywords: Muon-spin rotation; Organic magnet; Nanodisc; Quantum tunneling; Molecular magnet

1. Introduction

Muon-spin rotation (μSR) [1,2] has been extensively used in the study of various organic materials, including conducting polymers [3] and organic superconductors [4]. The technique has its most obvious application in the study of magnetic systems and is therefore ideally suited to studies of molecular magnetism. Muons are a *local* probe of internal fields, and therefore can be used to follow an order parameter as a function of temperature. Because 100% spin-polarized beams of muons can be prepared, the experiment does not need to be performed resonantly. The technique works very well in zero magnetic field and at milli-Kelvin temperatures (the incident muons easily pass through the dilution refrigerator windows). Muons provide information on antiferromagnets, spin-gap systems and spin glasses as well as on ferromagnets. If there are a range of muon sites it can provide information about internal magnetic field distributions. Studies can be performed of the magnetic fluctuations and spin dynamics, even above the magnetic transition temperature. Muons sensitively probe very weak magnetism sometimes found in heavy fermion systems [5] and therefore are demonstrably suitable for studying low-moment magnetism. In multi-phase samples, muons give signals proportional to the volume fraction of each phase, so they can be used to distinguish between a sample which is uniformly weakly magnetic and one which is non-magnetic but contains a tiny fraction of strongly magnetic impurity. This can be helpful in validating claims of authentic molecular magnets. In this paper, we present recent work using

* Corresponding author. Tel.: +44-1865-27-2347; fax: +44-1865-27-2400.
E-mail address: s.blundell@physics.ox.ac.uk (S.J. Blundell).

0277-5387/03/$ - see front matter
doi:10.1016/S0277-5387(03)00257-2

this technique on a variety of molecular magnetic systems.

2. The μSR technique

In our μSR experiments, a beam of almost completely spin-polarized muons was implanted with a momentum of 28 MeV/c into the sample under investigation. These stop quickly (in $<10^{-9}$ s), without significant loss of polarization. The observed quantity is then the time evolution of the muon-spin polarization, which can be detected by counting emitted decay positrons forward (f) and backward (b) of the initial muon-spin-direction; this is possible due to the asymmetric nature of the muon decay, which takes place in a mean time of 2.2 μs. In our experiments positrons are detected by using scintillation counters placed in front of and behind the sample. We record the number of positrons detected by forward (N_f) and backward (N_b) counters as a function of time and calculate the asymmetry function, $A(t)$:

$$A(t) = \frac{N_f(t) - \alpha N_b(t)}{N_f(t) + \alpha N_b(t)} \quad (1)$$

where α is an experimental calibration constant and differs from unity due to non-uniform detector efficiency. The quantity $A(t)$ is then proportional to the average muon-spin polarization, $P_z(t)$. The former quantity has a maximum value less than one since the positron decay is only preferentially, not wholly, in the direction of the muon-spin. $P_z(t)$ has a maximum value of one. The muon-spin precesses around a local magnetic field, B_i (with an angular frequency $\gamma_\mu|B_i|$, where $\gamma_\mu = 2\pi \times 135.5$ MHz T^{-1}).

If the local magnetic field at the muon site is at an angle of θ to the initial muon-spin-direction at the moment of implantation, the muon-spin will subsequently precess around the end of a cone of semi-angle θ about the magnetic field. The normalized decay positron asymmetry will be given by

$$P_z(t) = \cos^2\theta + \sin^2\theta\cos(\gamma_\mu|B_i|) \quad (2)$$

If the direction of the local magnetic field is entirely random then averaging over all directions would yield

$$P_z(t) = \frac{1}{3} + \frac{2}{3}\cos(\gamma_\mu|B_i|t) \quad (3)$$

which is plotted in Fig. 1(a). If the strength of the local magnetic field, $|B_i|$, is taken from a Gaussian distribution of width Δ/γ_μ centred around zero, then a straightforward averaging over this distribution gives

$$P_z(t) = \frac{1}{3} + \frac{2}{3}e^{-\Delta^2t^2/2}(1-\Delta^2t^2) \quad (4)$$

the Kubo-Toyabe relaxation function [6] (Fig. 1(b)). At short times, this relaxation function is Gaussian. The form of the relaxation can be calculated in the case of application of longitudinal magnetic field (Fig. 1(c)) and also for dynamics (Fig. 1(d)).

In the case of magnetic fluctuations, no spin precession signal can be observed, and so the muon polarization can be written

$$P_z(t) = P_z(0)e^{-\Gamma t} \quad (5)$$

The relaxation rate Γ is related to the field–field correlation function by

$$\Gamma = \int_0^\infty \gamma_\mu^2\langle B_\perp(t)B_\perp(0)\rangle\cos\omega_L t\,dt \quad (6)$$

where $\omega_L = \gamma_\mu B_L$ and B_L is the longitudinal field [7]. If $\langle B_\perp(t)B_\perp(0)\rangle = \langle B_\perp^2\rangle e^{-\nu t}$, where ν is the field–field correlation rate and $\langle B_\perp^2\rangle = 2(\Delta/\gamma_\mu)^2$ is the mean-square field at a given muon site, then

$$\Gamma = \frac{2\Delta^2\nu}{\nu^2 + \omega_L^2} \quad (7)$$

In particular, with no applied longitudinal field $\Gamma = 2\Delta^2/\nu$. The effect of the longitudinal field is to decouple the dynamical relaxation, so that $\Gamma \to 0$ when $\omega_L/\nu \to \infty$.

A range of coupling strengths Δ, such as might be found in a spin glass, can be modelled by a probability function [8]

$$\rho(\Delta) = \sqrt{\frac{2}{\pi}}\frac{a}{\Delta^2}e^{-a^2/2\Delta^2} \quad (8)$$

which is plotted in Fig. 1(e). Here $\langle\Delta\rangle$ scales with a. The muon relaxation function is then

$$P_z(t) = \int_0^\infty P_z(0)e^{-\Gamma t}\rho(\Delta)d\Delta = P_z(0)\exp(-(\lambda t)^{1/2}) \quad (9)$$

i.e. of 'root-exponential' form. The appropriate relaxation rate in this case is given by [7,8]

$$\lambda = \frac{2a^2\Gamma}{\Delta^2} = \frac{4a^2\nu}{\omega_L^2 + \nu^2} \quad (10)$$

and its field dependence is therefore as plotted in Fig. 1(f). In the following sections we present examples of the use of this technique to specific molecular magnetic systems.

3. Nitronyl nitroxides

Each molecule of the organic ferromagnetic *para*-nitrophenyl nitronyl nitroxide (*p*-NPNN) has a magnetic moment because of the radical (unpaired) electron which is delocalised over the O···N–C–N–O moiety. μSR experiments on *p*-NPNN (Fig. 2(a)) show the development of coherent spin precession oscillations below T_C [9]. The temperature dependence of the

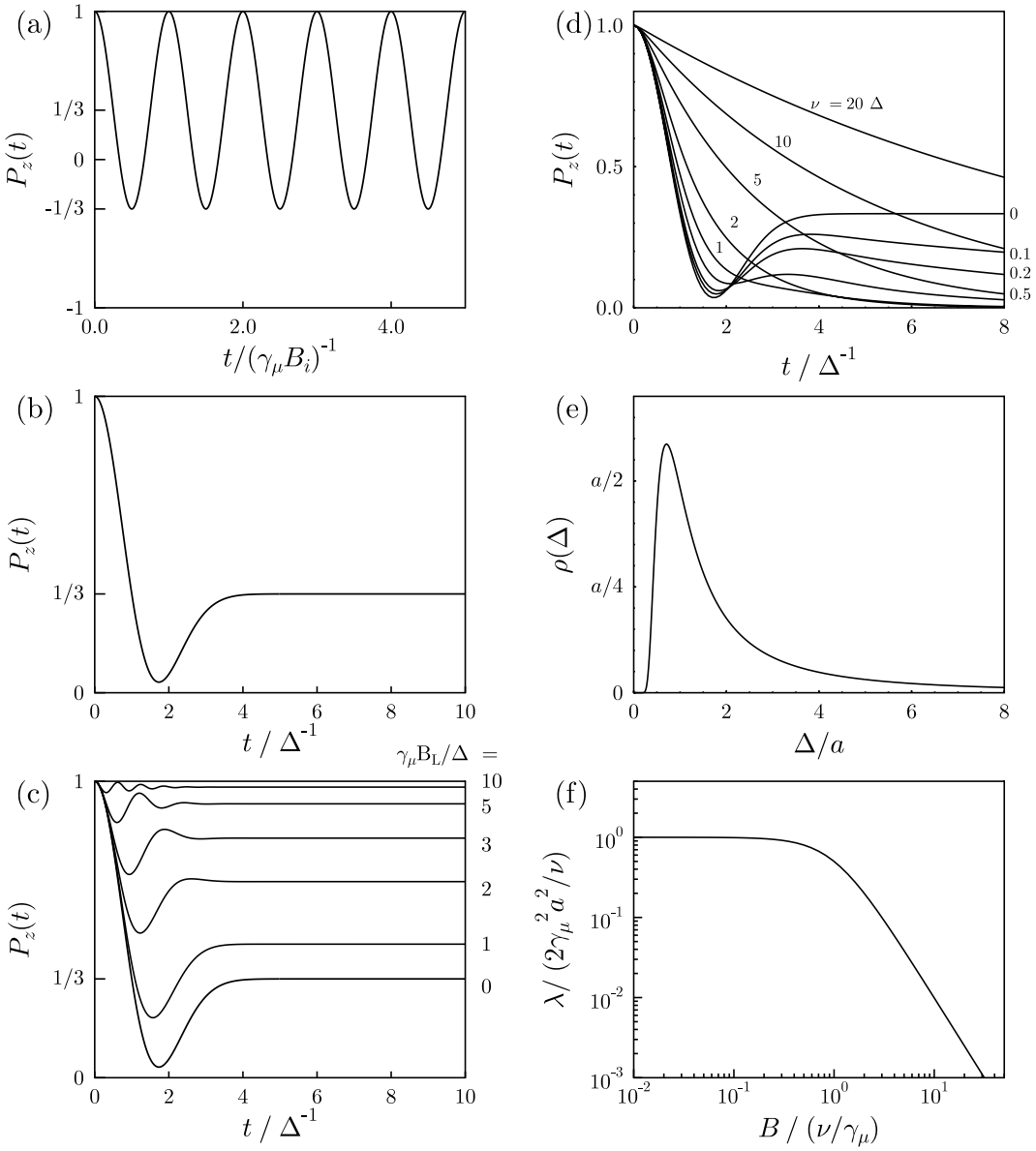

Fig. 1. (a) The muon relaxation function in Eq. (3). (b) The Kubo-Toyabe relaxation function (Eq. (4)). This is modified in the case of (c) a longitudinal field B_L and (d) dynamics with hop rate ν. (e) The probability distribution of coupling strengths Δ appropriate for a spin glass (Eq. (8)) and (f) the corresponding field dependence of the root-exponential relaxation rate (Eq. (10)).

precession frequency and the corresponding local field at the muon site is shown in Fig. 2(c). This is fitted to a functional form $\nu_\mu(T) = (1-(T/T_C)^\alpha)^\beta$ yielding $\alpha = 1.7 \pm 0.4$ and $\beta = 0.36 \pm 0.05$. This is consistent with three-dimensional long range magnetic order [9,10]. Near T_C the critical exponent is as expected for a three-dimensional Heisenberg model (one expects $\beta \approx 0.36$ in this case). At low temperatures the reduction in local field is consistent with a Bloch-$T^{3/2}$ law, indicative of three-dimensional spin waves.

Another molecular system, tanol suberate, is a biradical with formula $(C_{13}H_{23}O_2NO)_2$ and is found to be an antiferromagnet [11]. Each molecule contains two free radicals, with one unpaired electron localized on each of the N–O bonds, giving rise to a Curie–Weiss high temperature susceptibility. The specific heat exhibits a λ anomaly [11,12] at 0.38 K. μSR experiments [13] yield clear spin precession oscillations (see Fig. 2(b)). Although the oscillations look similar to those obtained for p-NPNN, the temperature dependence of the precession frequency (Fig. 2(c)) has a larger slope at low temperatures and fits to $\nu_\mu(T) = \nu_\mu(0)(1-T/T_C)^\beta$ where $\beta = 0.22$. This critical exponent is consistent with a two-dimensional XY magnet [14] and also with the temperature dependence of the magnetic susceptibility [15], suggesting that the ordered state is dominated by

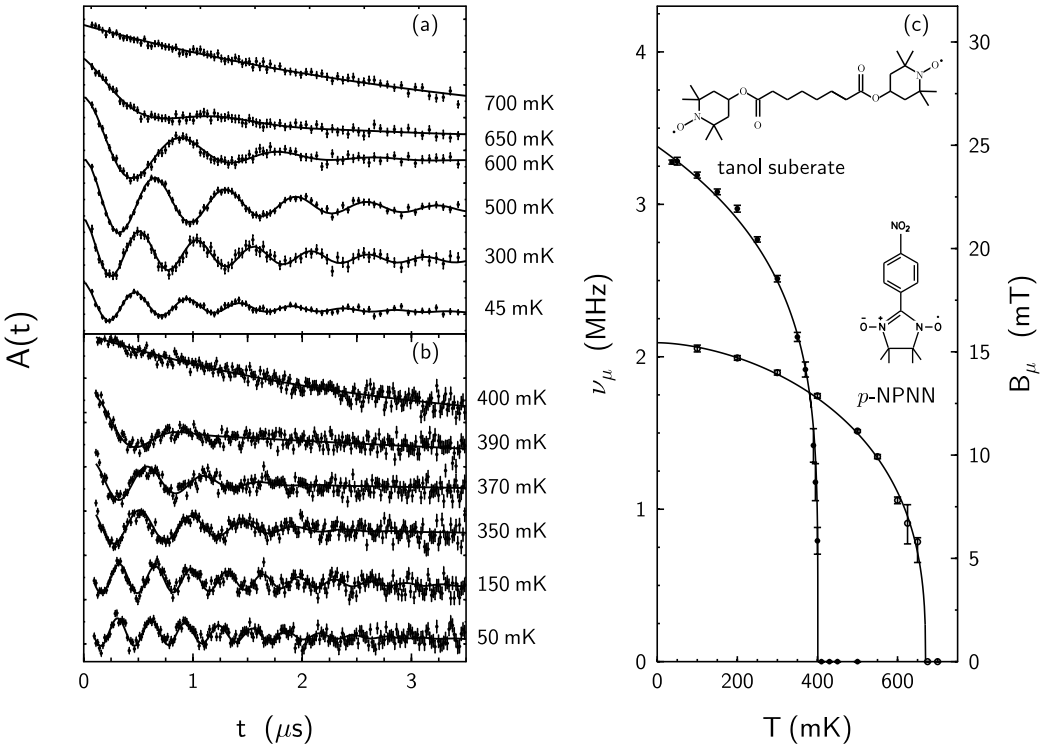

Fig. 2. Zero-field muon-spin rotation frequency in (a) the organic ferromagnet *p*-NPNN (after [9]) and (b) the organic antiferromagnet tanol suberate (after [13]). In both cases the data for different temperatures are offset vertically for clarity. (c) Temperature dependence of the zero-field muon-spin rotation frequency in *p*-NPNN and tanol suberate.

two-dimensional interactions. The relaxation rate of the oscillations rises to a maximum at the transition temperature and then falls dramatically. The coherent oscillations observed in both systems (and related ones [16]) in the ordered state demonstrate that the muons experience a homogeneous local field distribution and suggests a unique muon site.

Following muon implantation it is thought that muonium ($Mu = \mu^+ e^-$), with a single electronic spin, attaches to a particular nitronyl nitroxide and combines with the unpaired spin on the nitronyl nitroxide. The resulting electronic spin-state of the muoniated radical may be a singlet ($S = 0$, leading to a diamagnetic state) or a triplet ($S = 1$, leading to a paramagnetic state) [9]. Both states are found in experiments, the diamagnetic state giving rise to spin precession signals with frequency $\nu_\mu = (\gamma_\mu/2\pi)B_i$ in the internal field B_i, the paramagnetic states leading to extremely rapid precession in the hyperfine field, and hence to a loss of muon polarization at $t = 0$.

4. TDAE-C_{60}

The fullerene charge transfer salt (tetrakis(dimethylamino)ethylene)C_{60} (TDAE-C_{60}) is a ferromagnet with a transition temperature of 16 K [17], although there has been controversy about the nature of the ground state. It has recently been shown that fresh single crystals grown below 10 °C show no ferromagnetic behaviour when cooled down to 2 K (the α' phase) but on annealing at high temperature, they transform to the α phase which shows long range ferromagnetism below 16 K. The two forms appear structurally indistinguishable at room temperature, but small differences between the orientation of the C_{60} molecules in the two phases show up in structural data measured below 50 K [18]. In the α' phase the relative C_{60} orientations are similar to those encountered in other C_{60} solids with a hexagon on one

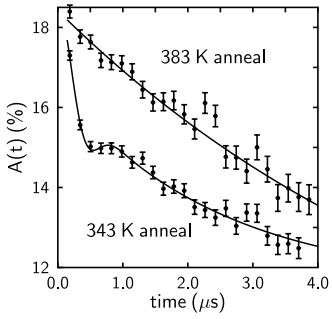

Fig. 3. Muon relaxation at 4 K in a sample of TDAE-C_{60} following annealing at 343 K and (subsequently) 383 K.

molecule facing the double-bond on another molecule. The α phase contains a new orientation, leading to various possible relative configurations.

Raw data at 4 K on a sample of TDAE-C_{60} are shown in Fig. 3 and show that a heavily damped spin precession signal is observable following annealing at 343 K for 4 hours. This signal is in agreement with an earlier μSR study [19] and the temperature dependence of the frequency of this signal is consistent with a Bloch-$T^{3/2}$ form [20]. The relaxation rate above T_C follows an activated temperature dependence. We find that the precession signal is destroyed following annealing at 383 K for 2 hours (in agreement with results obtained using ESR [21]) although we find a pronounced peak at 10 K in the relaxation rate in this state [20].

5. Spin crossover

A transition metal ion of configuration $3d^n$ ($n = 4$–7) in octahedral surroundings can have a low spin (LS) or high spin (HS) ground state, depending on the magnitude of the energy gap Δ between e_g and t_{2g} orbitals compared to the mean spin pairing energy P. When Δ and P are of comparable magnitude, the energy difference between the lowest vibronic levels of the potential wells of the two states may be sufficiently small that a change in spin-state may occur due to the application of a relatively minor external perturbation. A crossover [22,23] between the LS and HS states is associated with a change of magnetic properties and often by a change of colour. Iron (II) systems ($3d^6$) can show a crossover between LS ($S = 0$) and HS ($S = 2$) induced by changes in temperature or by light irradiation [24]. The crossover as a function of temperature is relatively smooth and gradual in solution, but very sharp in the solid state, showing that cooperativity plays an important rôle. The intermolecular interactions are thought to be communicated by phonons since the spin crossover is accompanied by a significant change in Fe-ligand bond-lengths [25,26].

The spin crossover can be followed using bulk measurements of the magnetic susceptibility χ as a function of temperature T. For Fe^{2+} ions, the molar fraction of molecules in the HS state, x, is given by $x = \chi T/(\chi T)_{HS}$ where $(\chi T)_{HS}$ is the value of χT when all molecules are in the HS state.

The spin crossover can be hysteretic so $T_c(\uparrow) \neq T_c(\downarrow)$ where $T_c(\uparrow)$ and $T_c(\downarrow)$ are the transition temperatures for warming and cooling, respectively. We have used implanted muons to study the spin crossover in two Fe(II) compounds: $Fe(PM\text{-}PEA)_2(NCS)_2$ ($T_c(\uparrow) = 231$ K, $T_c(\downarrow) = 194$ K) [27,28] and $Fe(PM\text{-}AzA)_2(NCS)_2$ ($T_c(\uparrow) = 192$ K, $T_c(\downarrow) = 186$ K) [29,30]. Susceptibility measurements on both samples shown a crossover from

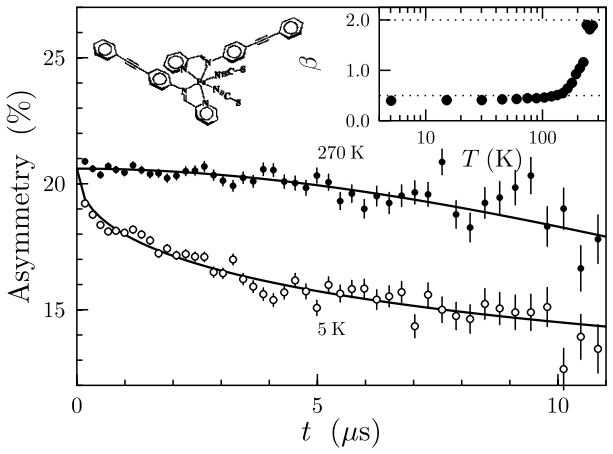

Fig. 4. Muon-spin relaxation in $Fe(PM\text{-}PEA)_2(NCS)_2$, (*cis*-bis(thiocyanato)bis(*N*-2′-pyridylmethylene)-4-(phenylethynyl) aniline iron), molecular structure shown in the left inset. The right inset shows the temperature dependence of β, which falls from 2 in the HS state to just below 1/2 in the LS state (the spin crossover is hysteretic; the data are taken on warming so that the appropriate crossover temperature is expected to be 231 K [30]).

a HS fraction x close to 1 at high temperatures to x close to 0 at low temperatures [29].

Data for the spin crossover compound $Fe(PM\text{-}PEA)_2(NCS)_2$ [27,31] are shown in Fig. 4. The asymmetry data $A(t)$ were fitted to a form

$$A(t) = A_{bg} + A_0 e^{-(\lambda t)^\beta} \tag{11}$$

where the background term A_{bg} and the relaxing

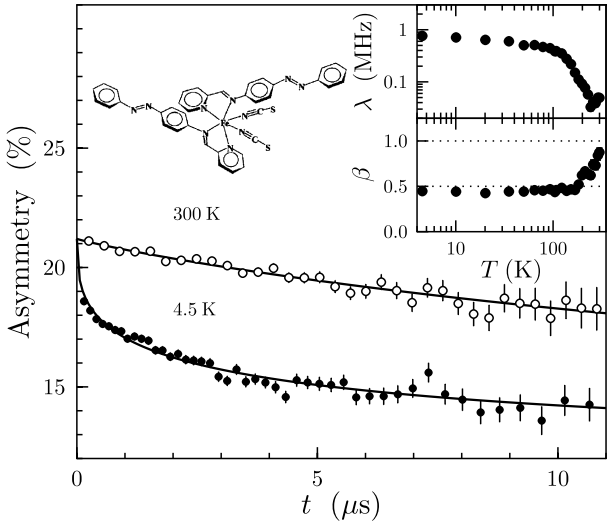

Fig. 5. Muon-spin relaxation in $Fe(PM\text{-}AzA)_2(NCS)_2$, (*cis*-bis(thiocyanato)bis(*N*-2′-pyridylmethylene)-4-(phenylazo) aniline iron), molecular structure shown in the left inset. The right inset shows the temperature dependence of λ and β. The parameter β falls from close to 1 in the HS state to just below 1/2 in the LS state (the data are taken on warming so that the appropriate crossover temperature is expected to be 192 K [30]).

amplitude A_0 were kept constant. The relaxation rate λ was only weakly temperature dependent so could be held constant in the fitting (at a value of 0.047 MHz, the average of fitted values when it was left free). The relaxation changes from Gaussian ($\beta = 2$) at temperatures above the spin crossover to root-exponential ($\beta = 0.5$) at low temperature, as shown in the inset to Fig. 4. Data for the spin crossover compound Fe(PM-AzA)$_2$(NCS)$_2$ [29,30] are shown in Fig. 5. In this case, the relaxation rate λ was quite strongly temperature dependent, so was not held constant in the fitting. The relaxation changes from close to exponential ($\beta = 1$) at temperatures above the spin crossover to root-exponential ($\beta = 0.5$) at low temperature, as shown in the inset to Fig. 5.

The muon interaction with a local moment is dominated by the dipole-dipole interaction, of the form $\mathscr{A}[S \cdot I - 3(S \cdot r)(I \cdot r)/r^2]$. In the HS state, all $S = 2$ moments will be fluctuating and exponential relaxation ($\beta = 1$) will result if the fluctuations are characterised by a single time constant τ and if the fluctuations are in the muon time-window. The relaxation rate $\lambda \propto \mathscr{A}^2\tau$ so that if τ is very short, $\lambda \to 0$ (motional–narrowing limit) and one may observe only relaxation due to static nuclear moments ($\beta = 2$).

In the LS state, for complete spin crossover, all the moments should disappear since all molecules are now $S = 0$ and one would again observe only nuclear moments ($\beta = 2$). However, for incomplete spin crossover, a few molecules will remain in the $S = 2$ state, even at very low temperatures. For a very dilute distribution of moments, fluctuating with a unique relaxation time τ, a 'root-exponential' ($\beta = 1/2$) relaxation is expected (because of the distribution in $\mathscr{A}$, see Section 2 above). In a more concentrated distribution of coupled moments found in certain spin glasses, a distribution in τ can result which leads to $\beta = 1/3$ [32,33].

For both Fe(PM-PEA)$_2$(NCS)$_2$ and Fe(PM-AzA)$_2$(NCS)$_2$ we observe muon-spin relaxation which is consistent with this picture [34]. In the HS state, the Fe $S = 2$ moments are uncoupled and fluctuate rapidly resulting in exponential relaxation for Fe(PM-AzA)$_2$(NCS)$_2$, but Gaussian relaxation for Fe(PM-PEA)$_2$(NCS)$_2$. This demonstrates that the fluctuations are much faster in Fe(PM-PEA)$_2$(NCS)$_2$ so that the muon-spin cannot follow them as the system is in the motionally narrowed limit. The residual relaxation is then Gaussian due to the static nuclear moments. The large temperature dependence of λ observed in Fe(PM-AzA)$_2$(NCS)$_2$ is also consistent with τ for this compound lying well within the muon time-window (but this is not the case for Fe(PM-PEA)$_2$(NCS)$_2$). The faster spin dynamics in Fe(PM-PEA)$_2$(NCS)$_2$ reflect the strong intrasheet and intersheet interactions which have been found by crystal structure determination [30]. In Fe(PM-AzA)$_2$(NCS)$_2$ the intersheet interactions are relatively weak. There is no structural phase transition at T_c (the space group is monoclinic $P2_1/c$ above and below T_c) for Fe(PM-AzA)$_2$(NCS)$_2$, but Fe(PM-PEA)$_2$(NCS)$_2$ undergoes a change of symmetry from monoclinic $P2_1/c$ HS to orthorhombic $Pccn$ LS [30], corresponding to a large rearrangement of the iron atom network. This symmetry change is responsible for the large hysteresis of the spin transition observed in Fe(PM-PEA)$_2$(NCS)$_2$.

In the LS state, most Fe moments become $S = 0$, but the spin transition is not complete and a dilute random distribution of $S = 2$ moments remains, leading to root-exponential relaxation in both cases [8]. In both cases, β settles to a value slightly below 1/2 so that we cannot rule out the spin glass type relaxation ($\beta = 1/3$) which results from a distribution in fluctuation times [32], although in either case the relaxation reflects a dilute distribution of fluctuating moments resulting from the incomplete spin transition.

6. Nanomagnets

Various chemically prepared magnetic clusters have recently attracted great interest as model systems for studying quantum effects such as the tunneling of the magnetic moment [35,36]. These systems are HS molecules; each molecule consists of a small network of magnetic ions coupled ferromagnetically or antiferromagnetically in such a way that the net spin of the cluster, S, is large. The reversal of the magnetic moment of a cluster is hindered by a strong Ising-type magnetic anisotropy. A magnetic field reduces the energy barrier, thus accelerating the dynamics. At high temperature, the anisotropy barrier is overcome by thermal activation and the relaxation is strongly temperature dependent. When the temperature is lower than the anisotropy barrier, the only possible spin-relaxation mechanism is quantum mechanical tunneling which is temperature-independent.

Recently some interesting disc-like molecular clusters about a nanometre across have been prepared which contain either 17 or 19 iron atoms linked by oxygen atoms with organic ligands arranged around the edge [37] (see the inset to Fig. 6(a)). μSR data [38] for the Fe_{19}-etheidi molecular cluster are shown in the inset to Fig. 6(b). The experiments were performed above the magnetic ordering temperature (1.07 K [39]). Root-exponential relaxation is found for all fields and temperatures studied, as found in experiments on related materials [40,41]. Since no recovery of the muon polarization is observed at long times, and since even fields of up to 0.39 T do not decouple the relaxation, we conclude that the cluster spins are dynamically fluctuating. The relaxation rate is strongly temperature dependent and increases as the temperature is cooled, but saturates at low temperature, as would be expected for a

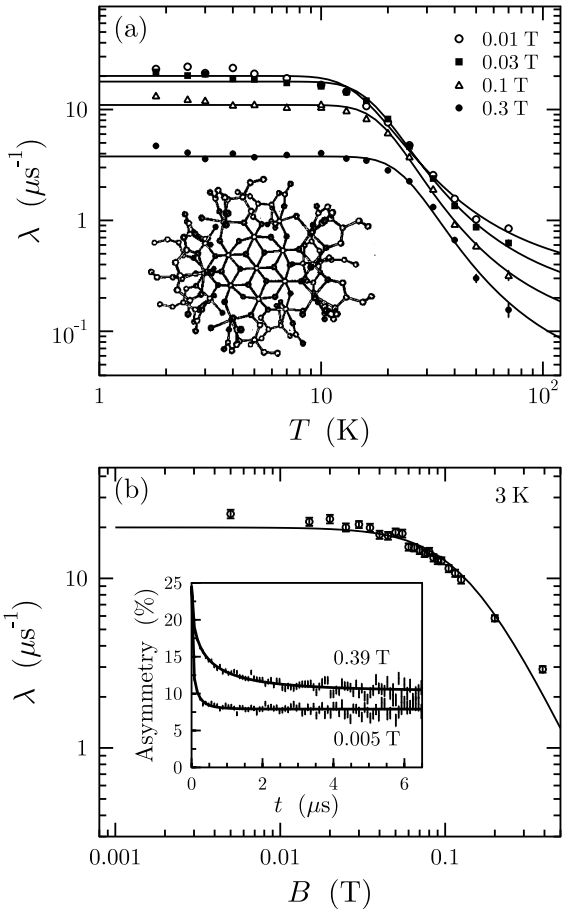

Fig. 6. (a) Temperature dependence of the muon-spin relaxation in Fe_{19} (etheidi)$_{10}$-$(OH)_{14}O_6(H_2O)_{12}$ at four values of the longitudinal field. The fits are as described in the text. The inset shows the molecular structure of the cluster. (b) Longitudinal field-dependence of the muon-spin relaxation at 3 K. The inset shows raw data at two fields (after [38]).

crossover from activated behaviour to quantum tunneling, though the crossover occurs at comparitively high temperature. The temperature dependence of the relaxation (Fig. 6(a)) contains a field-dependent term, λ_H, (responsible for the low-temperature plateaux, indicative of quantum fluctuations) and an activated term, $Ce^{-U/T}$. Following [40], we fit the relaxation to $\lambda = (\lambda_H^{-1} + Ce^{-U/T})^{-1}$. The fitted activation energy is found to be ~ 100 K and is very weakly field-dependent. Because of the multiple muon sites, the relaxation function is a root-exponential and the field dependence of the low temperature relaxation (Fig. 6(b)) can be fitted to Eq. (10). From this we find that the fluctuation rate ν is 113(6) MHz and the parameter a, the rms width of the distribution of $\sqrt{\langle B_\perp^2 \rangle}$, is 39(1) mT. Hence this would correspond to a tunneling rate $\tau^{-1} = \nu/2 = 57(3)$ MHz which is intermediate between that found for $CrNi_6$ and $CrMn_6$ [40]. Both $CrNi_6$ and $CrMn_6$ are isotropic ($D = 0$), whereas our disc-shaped material is anisotropic (for the related metheidi-based material, $D = -0.05$ cm^{-1} so that the anisotropy barrier is $D[(33/2)^2 - (1/2)^2] = 15.7$ K [37]; this is significantly lower than Mn_{12}Ac for which $S = 10$, $D = -0.46$ cm^{-1} [42] and the barrier is $DS^2 \approx 70$ K). The low temperature muon-spin relaxation in $CrNi_6$ and $CrMn_6$ has recently been ascribed to the hyperfine interaction [41] and it is possible that a related mechanism operates here. In order to distinguish between tunneling and hyperfine mechanisms, further work is needed on very similar systems in order to test whether the low temperature τ is independent of S or strongly dependent on S.

7. Conclusion

Our measurements have demonstrated that muons can be used to study magnetic order and dynamics in a variety of organic and molecular magnetic systems and to extract the fluctuation rate in HS molecules. We thank the EPSRC (UK) for financial support and the staff of the ISIS pulsed muon facility and the Paul Scherrer Institute for their valuable assistance and encouragement.

References

[1] S.J. Blundell, Contemp. Phys. 40 (1999) 175.
[2] P. Dalmas de Réotier, A. Yaouanc, J. Phys. C 9 (1997) 9113.
[3] F.L. Pratt, S.J. Blundell, W. Hayes, K. Ishida, K. Nagamine, A.P. Monkman, Phys. Rev. Lett. 79 (1997) 2855.
[4] S.L. Lee, F.L. Pratt, S.J. Blundell, C.M. Aegerter, P.A. Pattenden, K.H. Chow, E.M. Forgan, T. Sasaki, W. Hayes, H. Keller, Phys. Rev. Lett. 79 (1997) 1563.
[5] A. Amato, Rev. Mod. Phys. 69 (1997) 1119.
[6] R. Kubo, T. Toyabe, in: R. Blinc (Ed.), Magnetic Resonance and Relaxation, North-Holland, Amsterdam, 1967, p. 810.
[7] A. Keren, G. Bazalitsky, I. Campbell, J.S. Lord, Phys. Rev. B 6405 (2001) 4403.
[8] Y.J. Uemura, T. Yamazaki, D.R. Harshman, M. Senba, E.J. Ansaldo, Phys. Rev. B 31 (1985) 546.
[9] S.J. Blundell, P.A. Pattenden, F.L. Pratt, R.M. Valladares, T. Sugano, W. Hayes, Europhys. Lett. 31 (1995) 573.
[10] L.P. Le, A. Keren, G.M. Luke, W.D. Wu, Y.J. Uemura, M. Tamura, M. Ishikawa, M. Kinoshita, Chem. Phys. Lett. 206 (1993) 405.
[11] M. Saint Paul, C. Veyret, Phys. Lett. 45A (1973) 362.
[12] G. Chouteau, C. Veyret-Jeandey, J. Phys. 42 (1981) 1441.
[13] S.J. Blundell, A. Husmann, T. Jestadt, F.L. Pratt, I.M. Marshall, B.W. Lovett, M. Kurmoo, T. Sugano, W. Hayes, Physica B 289 (2000) 115.
[14] S.T. Bramwell, P.C.W. Holdsworth, J. Phys.: Condens. Mat. 5 (1993) L53.
[15] T. Sugano, S.J. Blundell, F.L. Pratt, T. Jestädt, B.W. Lovett, W. Hayes, P. Day, Mol. Cryst. Liq. Cryst. 334 (1999) 477.
[16] S.J. Blundell, I.M. Marshall, B.W. Lovett, F.L. Pratt, A. Husmann, W. Hayes, S. Takagi, T. Sugano, Hyp. Int. 133 (2001) 169.
[17] P.-M. Allemand, K.C. Khemani, A. Koch, F. Wudl, K. Holczer, S. Donovan, G. Gruner, J.D. Thompson, Science 253 (1991) 301.

[18] B. Narymbetov, A. Omerzu, V.V. Kabanov, M. Tokumoto, H. Kobayashi, D. Mihailovic, Nature 407 (2000) 883.
[19] A. Lappas, K. Prassides, K. Vavekis, D. Arcon, R. Blinc, P. Cevc, A. Amato, R. Feyerherm, F.N. Gygax, A. Schenck, Science 267 (1995) 1799.
[20] T. Lancaster, C. Steer, S.J. Blundell, F.L. Pratt, W. Hayes, A. Omerzu, D. Mihailovic, Synth. Met. 137 (2003) 1251.
[21] A. Mrzel, P. Cevc, A. Omerzu, D. Mihailovic, Phys. Rev. B 53 (1996) R2922.
[22] O. Kahn, Molecular Magnetism, Wiley-VCH, Weinheim, 1993.
[23] P. Gütlich, Y. Garcia, H.A. Goodwin, Chem. Soc. Rev. 29 (2000) 419.
[24] Y. Ogawa, S. Koshihara, K. Koshino, T. Ogawa, C. Urano, H. Takagi, Phys. Rev. Lett. 84 (2000) 3181.
[25] N. Willenbacher, H. Spiering, J. Phys. C 21 (1988) 1423.
[26] H. Spiering, N. Willenbacher, J. Phys.: Condens. Mat. 1 (1989) 10089.
[27] J.-F. Létard, P. Guionneau, E. Codjovi, O. Lavastre, G. Bravic, D. Chasseau, O. Kahn, J. Am. Chem. Soc. 119 (1997) 10861.
[28] H. Daubric, C. Cantin, C. Thomas, J. Kliava, J.F. Letard, O. Kahn, Chem. Phys. 244 (1999) 75.
[29] V. Ksenofontov, G. Levchenko, H. Spiering, F. Gütlich, J.-F. Létard, Y. Bouhedja, O. Kahn, Chem. Phys. Lett. 294 (1998) 545.
[30] P. Guionneau, J.-F. Létard, D.S. Yufit, D. Chasseau, G. Bravic, A.E. Goeta, J.A.K. Howard, O. Kahn, J. Mater. Chem. 9 (1999) 985.
[31] L. Capes, J.-F. Létard, O. Kahn, Chem. Eur. J. 6 (2000) 2246.
[32] I.A. Campbell, A. Amato, F.N. Gygax, D. Herlach, A. Schenck, R. Cywinski, S.H. Kilcoyne, Phys. Rev. Lett. 72 (1994) 1291.
[33] A.T. Ogielski, Phys. Rev. B 32 (1985) 7384.
[34] S.J. Blundell, C.A. Steer, F.L. Pratt, I.M. Marshall, J.F. Letard, Synth. Met. in press.
[35] E.M. Chudnovsky, J. Tejada, Macroscopic Quantum Tunneling of the Magnetic Moment, CUP, Cambridge, 1998.
[36] A. Caneschi, D. Gatteschi, C. Sangregorio, R. Sessoli, L. Sorace, A. Cornia, M.A. Novak, C. Paulsen, W. Wernsdorfer, J. Magn. Magn. Mater. 200 (1999) 182.
[37] J.C. Goodwin, R. Sessoli, D. Gatteschi, W. Wernsdorfer, A.K. Powell, S.L. Heath, J. Chem. Soc., Dalton Trans. (2000) 1835.
[38] S.J. Blundell, F.L. Pratt, T. Lancaster, I.M. Marshall, C.A. Steer, W. Hayes, T. Sugano, A. Caneschi, D. Gatteschi, J.F. Letard, S.L. Heath, Physica B 326 (2003) 556.
[39] M. Affronte, J. C. Lasjaunias, W. Wernsdorfer, R. Sessoli, D. Gatteschi, S. L. Heath, A. Fort, A. Rettori, Phys. Rev. B 66 (2002) 064408.
[40] Z. Salman, A. Keren, P. Mendels, A. Scuiller, M. Verdaguer, Physica B 289–290 (2000) 106.
[41] Z. Salman, A. Keren, P. Mendels, V. Marvaud, A. Scuiller, M. Verdaguer, J.S. Lord, C. Baines, Phys. Rev. B 65 (2002) 132403.
[42] D. Gatteschi, P. Carretta, A. Lascialfari, Physica B 289 (2000) 94.